Dual Drug-Loaded Biofunctionalized Amphiphilic Chitosan Nanoparticles: Enhanced Synergy between Cisplatin and Demethoxycurcumin against Multidrug-Resistant Stem-Like Lung Cancer Cells

Wei-Ting Huang [a], *Mikael Larsson* [b,c], *Yi-Chi Lee* [a], *Dean-Mo Liu* [a,*], *Guang-Yuh Chiou* [d*]

[a] Department of Materials Science and Engineering, National Chiao Tung University, 1001 Ta-Hseuh Road, Hsinchu City, Taiwan 300, ROC.

[b] School of Energy and Resources, University College London, 220 Victoria Square, Adelaide, SA 5000, Australia.

[c] Future Industries Institute, University of South Australia, Mawson Lakes Campus, SA 5095, Australia.

[d] College of Biological Science and Technology, National Chiao Tung University, 1001 Ta-Hseuh Road, Hsinchu City, Taiwan 300, ROC.

*** Corresponding Authors:**

D.M. Liu: P: +886 3 571 2121 ext. 55391; F: +886 3 572 4727; Email: deanmo.liu@gmail.com

y@hotmail.com

ABSTRACT: Lung cancer kills more humans than any other cancer and multidrug resistance (MDR) in cancer stem-like cells (CSC) is emerging as a reason for failed treatments. One concept which addresses this root cause of treatment failure is the utilization of nanoparticles to simultaneously deliver dual drugs to cancer cells with synergistic performance, easy to envision — hard to achieve. It is challenging to simultaneously load drugs of highly different physicochemical properties into one nanoparticle, release kinetics may differ between drugs and general requirements for biomedical nanoparticles apply. Here self-assembled nanoparticles of amphiphilic carboxymethyl-hexanoyl chitosan (CHC) were shown to present nano-microenvironments enabling simultaneous loading of hydrophilic and hydrophobic drugs. This was expanded into a dual-drug nano-delivery system to treat lung CSC. CHC nanoparticles were loaded/chemically modified with the anticancer drug cisplatin and the MDR-suppressing Chinese herbal extract demethoxycurcumin, followed by biofunctionalization with CD133 antibody for enhanced uptake by lung CSC, all in a feasible one-pot preparation. The nanoparticles were characterized with regard to chemistry, size, zeta potential and drug loading/release. Biofunctionalized and non-functionalized nanoparticles were investigated for uptake by lung CSC. Subsequently the cytotoxicity of single and dual drugs, free in solution or in nanoparticles, was evaluated against lung CSC at different doses. From the dose response at different concentrations the degree of synergy was determined through Chou-Talalay's Plot. The biofunctionalized nanoparticles promoted synergistic effects between the drugs and were highly effective against MDR lung CSC. The efficacy and feasible one-pot preparation suggest preclinical studies using relevant disease models to be justified.

KEYWORDS: biodegradable chitosan nanoparticle; CD133; CDDP; dual-drug delivery; synergistic effect

1. Introduction

Amphiphilic carboxymethyl-hexanoyl chitosan (CHC) was modified through a feasible one-pot preparation to achieve antibody-functionalized dual-drug nanoparticles for simultaneous delivery of demethoxycurcumin (DMC) and cisplatin (CDDP). It was hypothesized that the simultaneous intracellular delivery and co-localization of the drugs mediated by the nanoparticles would result in greatly enhanced synergistic effect against lung cancer stem-like cells (CSC) and that this nanomedical technology would thus show potential for combinatorial cancer therapy, an approach already employed in treatment of lung cancer by clinicians using free drugs [1].

Among cancers, lung cancer remains a leading killer [2]. Treatment of non-small cell lung cancer (NSCLC) is particularly important from a healthcare perspective, as it combines high prevalence (about 85% of lung cancer cases) with high mortality [2]. When the cancer has entered the stage at which complete removal by surgery is difficult, chemotherapy, targeted drugs or immunotherapy is commonly employed [2]. Unfortunately the 5-year survivability is quite low, even with treatment [2]. The difficulty in killing of the cancer and the resulting low survival rate may be due to CSC [3, 4]. The role of CSC is just beginning to be understood, but they are thought to play critical roles in metastasis and cancer relapse after treatment, while also presenting multidrug resistance (MDR) features [3, 4]. It is thus critical to develop improved treatments to overcome MDR and effectively kill the CSC.

Dual-drug administration has been discussed for years as a means to improved cancer treatment with potential benefits such as reduced side-effects due to lowering of drug concentrations and reduction of MDR. Although nanoparticle-based dual-drug delivery seems

highly promising, there are challenges in terms of complex production processes, low encapsulation efficiencies and unfavorable release profiles of the different drugs [5].

In the clinic, CDDP is a first-line drug for NSCLC treatment and combinations with other drugs are commonly employed [1]. However, resistance of cancers towards CDDP is commonly observed through cysteine-rich protein blocking [6, 7] and responses from the NF-κB-upregulated MDR CD133 signaling pathway, which is highly active in CSC [3, 6, 8-10]. Cells with upregulated CD133 present resistance to treatment, self-renewal capability, fast DNA repair and overexpression of multidrug resistance protein 1 (MRP1) and breast cancer resistance protein 1 (BCRP), among others [3, 8, 10]. Curcuminoids, a traditional Chinese medicine herbal extract, have been reported to downregulate NF-κB, inhibit MDR-related proteins, promote apoptosis through inactivation of Bcl-2 [11, 12] and reverse CDDP resistance in lung cancer [13]. Recently, free curcumin has also been shown to act in synergy with CDDP and CDDP/polymer-conjugate nanoparticles to achieve improved efficacy against CDDP-resistant ovarian cancer cells [14]. DMC is a curcuminoid with better stability in blood and under basic condition compared to the commonly used curcumin [15]. Therefore, this work focused on feasible one-pot preparation of CD133-antibody dressed nanoparticles for simultaneous intracellular delivery of the well-proven hydrophilic anticancer drug CDDP and the hydrophobic curcuminoid DMC to overcome MDR in CSC through enhanced synergistic effects. *In vitro* evaluation of cell internalization and effectiveness against MDR lung cancer cells was carried out using A549-ON, a stable cell line presenting stem-like characteristics and overexpression of CD133, prepared by transfection of human A549 lung adenocarcinoma cells using a lentiviral infection system with vectors encoding *Oct4* and *Nanog* cDNA [9].

2. Methods

2.1. Materials

Cis- diammine platinum(II) dichloride (cisplatin, CDDP), o-phenylenediamine (OPDA), dimethyl sulfoxide (DMSO), 1-ethyl-3-(3-dimethylaminopropyl)carbodiimide hydrochloride (EDC), 3-(4,5-Dimethylthiazol-2-yl)-2,5-diphenyltetrazolium bromide (MTT), 2-propanol, sodium hydroxide, chloroacetic acid, deuterium oxide (D_2O), and phosphate buffered saline (PBS) were purchased from Sigma-Aldrich. Carboxymethyl-hexanoyl chitosan (CHC) was purchased from Advanced Delivery Technologies, Inc. PSVue®480 was purchased from Molecular Targeting Technologies, Inc. N,N-dimethylformamide (DMF) was purchased from Aencore. Demethoxycurcumin (DMC) was a courteous gift from China Medical University (Taiwan). The CD-133 antibody was purchased from Genetex. All other chemical reagents in the study were of analytical grade and were used as received without further purification. A549-ON, a stable cell line with stem-like characteristic and overexpression of CD133, prepared by transfecting human A549 lung adenocarcinoma cells using a lentiviral infection system with vectors encoding *Oct4* and *Nanog* cDNA [9], were kindly provided by Professor Shih-Hwa Chiou (Yang Ming University, Taiwan). The reader is referred to the given reference for detailed cell characteristics and preparation protocol.

2.2. Preparation of CHC/CDDP and CHC/DMC Nanoparticles:

CHC/CDDP and CHC/DMC nanoparticles were prepared by mixing 0.4 mL of CDDP or DMC (1 mg/mL) in 1% DMSO in ddH_2O with 1 mg of CHC and 1.6 mL pH 11 ddH_2O. The pH of the resulting solution was about 7 and the particles were mixed on a magnetic stirrer for 12 h to allow self-assembly into drug loaded nanoparticles. Subsequently, the sample was placed into Amincon centrifugal filter and centrifuged at 5000 rpm for 30 minutes to remove unloaded drug.

The gel-like nanoparticle-concentrate was dispersed ddH_2O to required concentrations. Encapsulation efficiency (EE) was measured, as described in section 2.6, before use of nanoparticles to ensure use of correct drug concentration.

2.3. Analysis of CHC/CDDP Interactions:

Fourier transformed infrared spectroscopy (FT-IR) was conducted on a Spectrum 100 (Perkin Elmer) as follows: 1 mL samples nanoparticle samples were concentrated using Amicon centrifugal filters under 5000 rpm for 30 minutes. Subsequently, 100µL of ddH_2O was added to disperse the nanoparticle-concentrates. The nanoparticle dispersions were applied on silicon wafers, taking care to avoid bubble formation, and were dried at 50 ^oC. Spectra were recorded with a resolution of 1 cm^{-1} between 4000 and 400 cm^{-1}.

Samples for X-ray photoelectron spectroscopy (XPS) analysis were prepared as follows: Nanoparticle dispersions were freeze-dried for one day to obtain fiber-like samples that were mounted on silicon wafers. CDDP powder was mounted as delivered onto the silicon wafer. The samples were briefly sputtered with Au to improve the electrical conductivity and were analyzed for elemental composition using a Microlab 350 X-ray photoelectron spectrometer (VG Scientific) equipped with Mg Kα source.

Samples were prepared for platinum nuclear magnetic resonance spectroscopy (^{195}Pt NMR) by freeze-drying of 10 mL of dissolved CDDP or dispersed nanoparticles for one day, followed by dissolution/dispersion in 1 mL of D_2O. ^{195}Pt NMR spectra were recorded using a 600 MHz Mercury NMR spectrometer (Varian).

2.4. Preparation of CHC/DMC-CDDP Nanoparticles:

CHC/CDDP-DMC nanoparticles were prepared by mixing 0.4 mL of DMC (X µg/mL) in 1% DMSO in ddH_2O with 1 mg of CHC and 1.2 mL pH 9 ddH_2O, followed by addition of 0.4 mL of

CDDP (Y µg/mL) in 1% DMSO in ddH_2O. For characterizations and *in vitro* release X and Y = 1000. To investigate the effect of different drug concentrations on *in vitro* cytotoxicity the drug loading was modified to achieve desired concentrations (X, Y = 50, 750; 100, 1500; 150, 2250; 150, 3000; 200, 3000). The pH of the resulting solution was about 7 and the particles were mixed on a magnetic stirrer for 12 h to allow self-assembly into drug loaded nanoparticles. Further preparation was performed as for CHC/CDDP nanoparticles, described above. Before use the EE was measured for each preparation, as described in section 2.6, to ensure use of correct drug concentrations.

2.5. Modification with CD133 Antibodies:

After preparing CHC/CDDP-DMC nanoparticles, as described above, but before the centrifugation-filtration step to separate nanoparticles from free drug, 1 µL of anti-CD133 antibodies (1 mg/mL in ddH_2O) was added to the solution. The mixture was stirred at 4 ^oC for one hour, after which 0.05 mL of EDC solution (0.1%, w/v) was slowly added over 4 hours to crosslink between carboxyl groups and amine groups. The CHC/CDDP-DMC/Anti-CD133 nanoparticles were subsequently separated from free drug and unreacted reagents using an Amicon centrifugal filter at 5000 rpm for 30 minutes. As for non-targeted nanoparticles, the gel-like concentrate was dispersed in ddH_2O to a final volume of 2 mL.

2.6. Encapsulation Efficiency of CHC-Based Nanoparticles:

The drug EE was calculated using Eq 1:

$$EE\% = \frac{A}{B} \times 100\% \quad (1)$$

where A is the amount of drug loaded in nanoparticles and B is the total amount of added drug.

For cisplatin, quantification of drugs in nanoparticles and free drug was performed using inductively coupled plasma mass spectrometry (ICP-MS) and UV-Visible spectroscopy after

reaction with OPDA [16]. Amicon centrifugal filters were used to separate free drug from drug loaded in nanoparticles by centrifugation at 5000 rpm for 30 min. The filtrate was collected and the amount of free drug was determined by UV-Visible spectroscopy after addition of an equal volume of 1.4 mg/mL OPDA solution in presence of DMF and heating at 100 ^{o}C for 30 min. The resulting light-blue platinum-OPDA complex was detected at 705 nm by UV-Visible spectroscopy. ICP-MS analysis of the platinum concentration was conducted using a JY-24 Sequential Spectrometer (Jobin Yvon) [17]. For DMC, the amounts of nanoparticle-loaded and free drug were determined though high-performance liquid chromatography (HPLC) on a 1200 series HPLC system (Agilent Technologies) with a C18 column (Zorbax eclipse, 5 µm, 4.6 × 150mm). Eluted DMC was detected at 425 nm using a Spectra100 UV−vis detector.

2.7. Characterization of Nanoparticles:

The size and zeta potential of nanoparticles in PBS buffer were determined by dynamic light scattering (DLS) and zeta potential analysis using a Beckman Coulter DLS instrument. The morphology of dried nanoparticles was examined using a JEOL 6700 scanning electron microscope (SEM). Samples for SEM were prepared by diluting nanoparticle suspension immediately after preparation to 0.05% (w/v) with ddH_2O and placing a drop on a clean silicon wafer, followed by drying and platinum sputtering. Transmission electron microscopy (TEM) analyzes were conducted using a JEOL 2100. Samples for TEM were prepared by diluting the nanoparticle suspension immediately after preparation to 0.1% (w/v) with ddH_2O, followed by application to a carbon-coated 200-mesh copper grid.

2.8. In vitro Release of DMC and CDDP from CHC-Based Nanoparticles:

In vitro drug release tests were conducted by dissolving nanoparticles in PBS at pH 5.5 and pH 7.4 (final concentration of DMC, CDDP and CHC was 100 µg/mL, 200 µg/mL and 0.05 wt%,

respectively). The solutions were divided into 1.5 mL Eppendorf tubes, 3 for each time point. The tubes were gently shaken at 37 ^{o}C in an orbital shaker incubator. At predetermined times (4, 8, 12, 24, 42 and 48 h) the released (free) drugs were separated from nanoparticles loaded with drugs by centrifugation. For DMC samples were centrifuged at 1000 rpm for 2 min and the pellet consisting of the precipitated released DMC was analyzed. For CDDP samples were filtered using Amicon centrifugal filters at 5000 rpm for 30 minutes and the filtrate containing released CDDP was analyzed. The concentrations of DMC and CDDP were quantified by HPLC and ICP-MS, as described above in the encapsulation efficiency section. The percentages of DMC and CDDP released at each time were calculated from the following equation:

Released drug (%) = [(released drug) / (initial amount of drug)] X100 (2)

2.9. Cell Culture:

A549-ON and A549 cells were cultured in DMEM medium with 10% fetal bovine serum and were incubated under 5% CO_2 and 37 ^{o}C [9]. The culture medium was renewed every two days and the cells were sub-cultured by trypsin-EDTA treatment.

2.10. Cellular Uptake

Cell internalization of nanoparticles by A549-ON and A549 cells was analyzed as follows. The investigated nanoparticles were loaded with the hydrophobic fluorescent reporter substance PSVue, which due to its hydrophobicity enters the CHC nanoparticles. 10^6 cells were plated in a 100 mm dish and were allowed to attach for 24 hrs. To examine the effect of incubation time on nanoparticles internalization, the cells and nanoparticles (at 0.05 wt% CHC concentration) were suspended together in the medium for various time times (0.5, 1, 2, 4 h) at 37 °C. Free or nanoparticle loaded PSVue was used at a concentration of 100 μg/mL. After the incubation the cells were washed twice with PBS and were collected by trypsinization. Subsequently the cells

were centrifuged, dehydrated with 70% ethanol overnight at -20 °C and re-suspended in PBS at 10^6 cells/mL. To avoid cell aggregation, the cell solutions were filtered through a nylon membrane (BD Biosciences, USA). The cellular uptake of PSVue was determined using a BD FACS Calibur flow cytometer (BD Biosciences) and the fluorescence intensity was quantified with CellQuest Pro software (BD Biosciences). A minimum of ten thousand cells were analyzed.

2.11 In Vitro Cytotoxicity

The cytotoxicity of DMC, free CDDP, free DMC and CDDP combo, CHC/DMC nanoparticles, CHC/CDDP nanoparticles, CHC/DMC-CDDP nanoparticles and CHC/DMC-CDDP/anti-CD133 nanoparticles against A549-ON and A549 cells was evaluated by MTT colorimetric assay as follows: Cells were plated at 2×10^4 cells per well in a 24-well culture plate (Corning, USA) for attachment, followed by replacement of the medium with drug containing medium and incubation for 24h. Subsequently the medium was removed and the wells were washed twice with PBS. Then, MTT solution (0.5 mg/mL) was added followed by incubation for 4 h. The purple formazan was solubilized with isopropanol and cell viability was assessed by measuring the absorbance at 595 nm using a microplate reader (TECAN Sunrise, Switzerland).

For A549-ON cells, the following drug dosages were used: Free drugs (as single or dual drug solution) [DMC] = 0, 3.25, 7.5, 15 and 20 µg/mL, [CDDP] = 0, 75, 150, 300 and 600 µg/mL; CHC/DMC nanoparticles [DMC] = 2.5, 5, 10, 15, and 20 µg/mL; CHC/CDDP nanoparticles [CDDP] = 50, 100, 200, 400, 800 µg/mL; CHC/DMC-CDDP and CHC/DMC-CDDP/anti-CD133 nanoparticles [DMC] = 0, 1.25, 3, 5, 6 and 9 µg/mL, [CDDP] = 0, 95, 125, 200, 250, 265 µg/mL.

For A549 cells, the following drug dosages were used: Free drugs (as single drug solution) [DMC] = 0, 3.25, 7.5, 15 and 20 µg/mL, [CDDP] = 0, 12.5, 25, 50, 100 and 200 µg/mL; Free

drugs (as dual drug solution) [DMC] = 0, 1.25, 2.5, 5 and 10 µg/mL, [CDDP] = 0, 25, 50, 75 and 100 µg/mL; CHC/DMC nanoparticles [DMC] = 2.5, 5, 10, 15, and 20 µg/mL; CHC/CDDP nanoparticles [CDDP] = 0, 12.5, 25, 50, 100 and 200 µg/mL; CHC/DMC-CDDP nanoparticles [DMC] = 0, 1.25, 2.5, 5 and 10 µg/mL, [CDDP] = 0, 25, 50, 75 and 100 µg/mL.

Cytotoxicity data was analyzed to determine IC_{50} and synergy using CompuSyn and and Chou-Talalay's Plot, as described in literature [18].

3. Results

3.1. Preparation of CDDP-Loaded CHC Nanoparticles and Characterization of CHC-CDDP Interactions

It has been previously shown that cyto- and biocompatible [19, 20] CHC can effectively encapsulate and deliver DMC to lung cancer cells [21]. Thus the initial focus was to establish effective loading/modification of CHC with CDDP. Simple mixing of CDDP in 1% DMSO in ddH_2O with CHC in ddH_2O at pH 7 resulted in CDDP-loaded nanoparticles (CHC/CDDP) with EE of up to 65%, as determined by ICP-MS. XPS analysis confirmed the presence of CDDP in the nanoparticles. The shift of the Pt 4f peak towards higher binding energies (Fig. 1A, B) and the decrease in Cl:Pt ratio from about 2 for CDDP to about 1 for CHC/CDDP indicated binding of CDDP with CHC through replacement of chlorine in CDDP with a bond to oxygen, as described in literature [22]. The bond formation was further supported by changes in FTIR spectrum, where in particular the C-O stretch at 1209 cm^{-1} in CHC disappeared for CHC/CDDP (Fig. 1C).

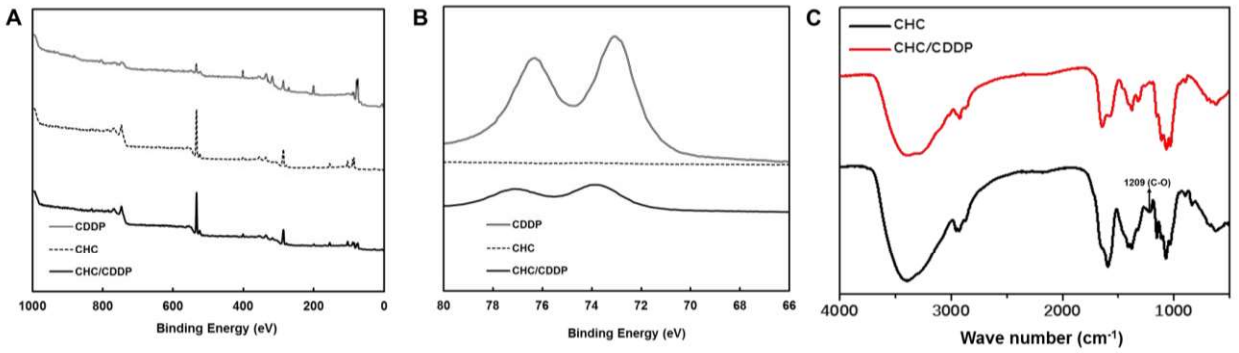

Fig. 1. Confirmation of chemical bond formation in CHC/CDDP through XPS and IR. (A) XPS spectra of free CDDP, CHC and CHC/CDDP. (B) Pt signals at 74 eV and 78 eV from XPS analysis of free CDDP, CHC, and CHC/CDDP. (C) IR spectra of CHC and CHC/CDDP.

Additional evidence for the formation of a chemical bond between CDDP and CHC through replacement of chlorine with oxygen was provided by ^{195}Pt NMR, where chemical shifts of 2101 ppm and 1849 ppm were recorded for CDDP and CHC/CDDP, respectively (Fig. 2), in agreement with literature [23, 24]. Combined the results prove that CDDP formed bonds with the carboxylic acid oxygen of CHC through replacement of chlorine.

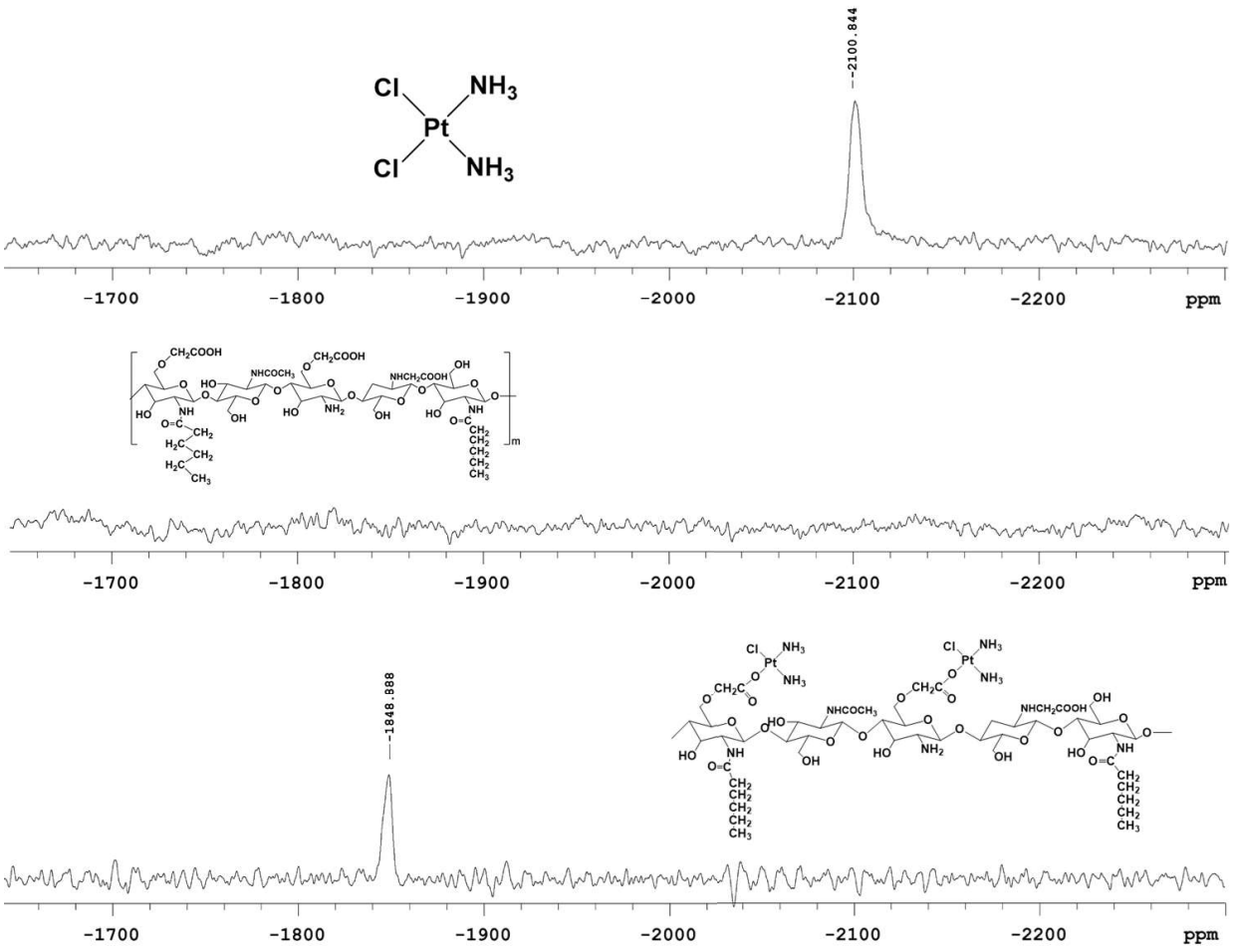

Fig. 2. ^{195}Pt NMR (600 MHz) analysis of CDDP, CHC and CHC/CDDP in D_2O. Recorded chemical shifts were 2101 ppm for CDDP and 1849 ppm for CHC/CDDP. No signal was observed for pure CHC.

3.2. Preparation and Characterization of Single/Dual-Drug Loaded and Biofunctionalized CHC Nanoparticles

Nanoparticles incorporating both DMC and CDDP (CHC/DMC-CDDP) were again prepared by simple mixing of the drugs in 1% DMSO in ddH_2O with CHC in ddH2O at pH 7, resulting in

EE of up to 50% and 60% for DMC and CDDP, respectively. Surface modification with CD133-antibodies to form CHC/DMC-CDDP/anti-CD133 nanoparticles was achieved by addition of the antibodies, mixing at 4 ^{o}C and addition of EDC crosslinker followed by further mixing, all in one pot without purification steps. See Scheme 1 for conceptual drawing of the process.

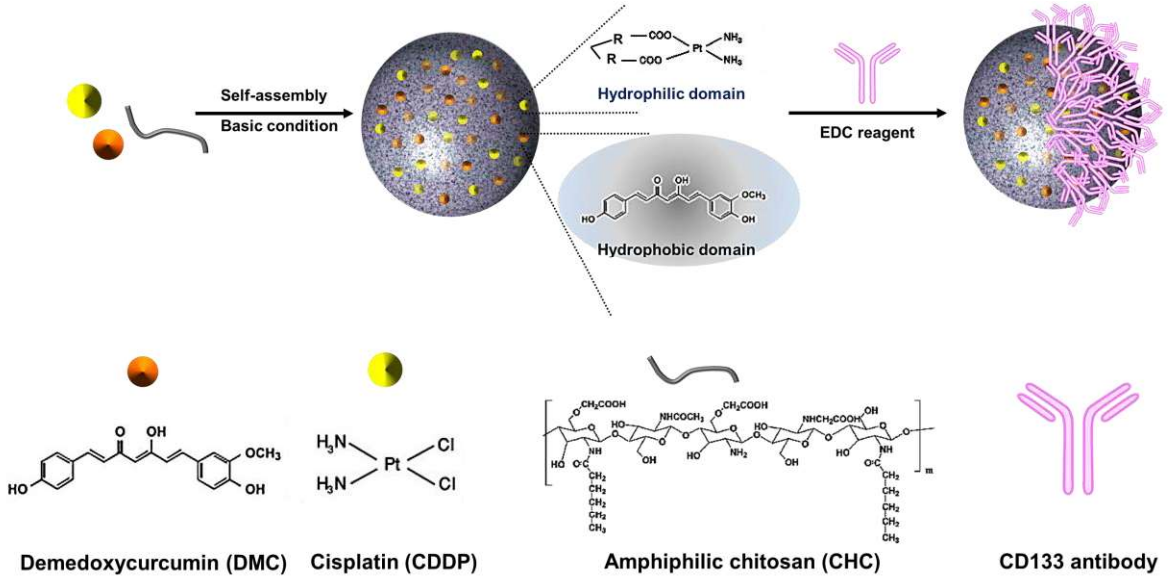

Scheme 1. Drawing illustrating the components and steps involved in the one-pot preparation of CHC/DMC-CDDP/anti-CD133 nanoparticles.

TEM analysis revealed sub-100 nm sizes of bare CHC and CHC/CDDP nanoparticles, while nanoparticles containing DMC were above 100 nm in size. It was also found that CDDP alone distributed in nanometer-sized clusters through the CHC nanoparticle. Furthermore, CHC/DMC-CDDP/anti-CD133 nanoparticles presented a distinct core loaded with CDDP and DMC and a shell-like feature seemingly without drugs (Fig. 3A-C; additional TEM images in supplementary material Fig. S1). SEM confirmed the CHC/DMC-CDDP/anti-CD133 nanoparticles to have a narrow size distribution in the 100-200 nm range (Fig. 3D). The nanoparticle sizes observed

using electron microscopy agreed well with those acquired in PBS using DLS for each preparation (Table 1). The anti-CD133 modified particles presented a slight negative zeta potential (≈ -3 mV in PBS, see Table 1 for details on zeta potential for each preparation) while maintaining good colloidal stability.

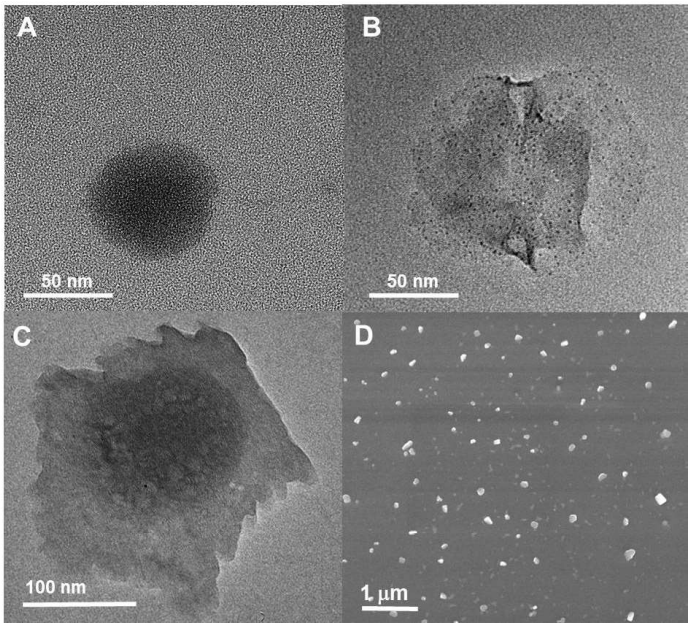

Fig. 3. Electron microscopy images of different nanoparticle preparations. TEM image of individual nanoparticle for (A) CHC, (B) CHC/DMC-CDDP, (C) CHC/DMC-CDDP/anti-CD133. (D) SEM image of CHC/DMC-CDDP/anti-CD133 nanoparticles.

Table 1. Hydrodynamic diameter from DLS and zeta potential of different formulations in pH 7.4 PBS. One standard deviation is given within parentheses (n = 3).

Sample	D (nm)	Zeta Potential (mV)
CHC	50 (10)	-22 (0.65)
CHC/DMC	130 (21)	-9 (1.1)

CHC/CDDP	75 (12)	-21 (2.7)
CHC/DMC-CDDP	150 (20)	-6 (2.3)
CHC/DMC-CDDP/anti-CD133	190 (17)	-3 (1.0)

3.3 In Vitro Drug Release

The *in vitro* release of CDDP and DMC from different preparations in pH 5.5 (relevant to lysosomes) and pH 7.4 PBS buffer was determined over 48 h. As seen in Fig. 4 there was a general trend that dual-drug loading and anti-CD133 modification reduced the drug release rate and the amount of drug released at the plateaus in the release curves. The exception was the release of CDDP at pH 5.5, which was similar for all preparations. For the CHC/DMC-CDDP/anti-CD133 nanoparticles, being the preparation in focus, only about 10% of DMC and 14% of CDDP was released over the 48 h of the experiment at pH 7.4. At pH 5.5 the corresponding numbers were about 20% and 30% for DMC and CDDP, respectively.

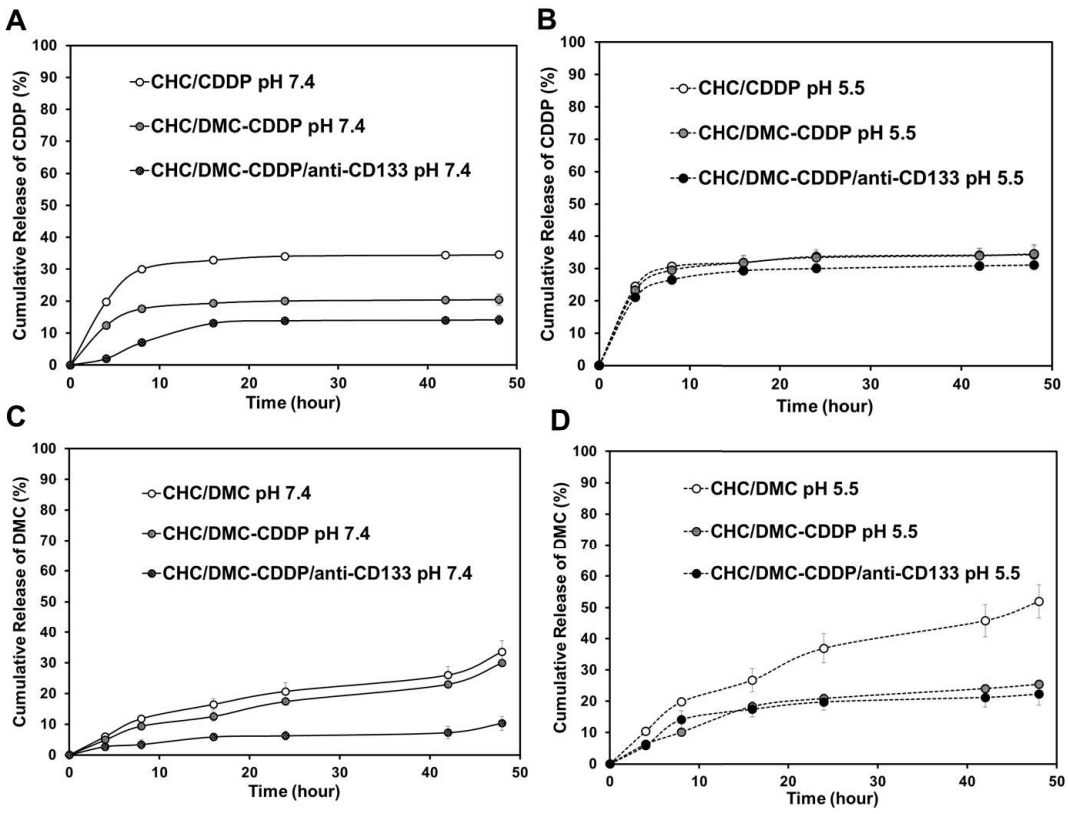

Fig. 4. *In vitro* cumulative release profile of DMC and CDDP from CHC/DMC, CHC/DMC-CDDP and CHC/DMC-CDDP/anti-CD133 nanoparticles in PBS buffer with pH 5.5 or 7.4 at 37 ^{o}C; (A) DMC - pH 7.4, (B) DMC - pH 5.5, (C) CDDP - pH 7.4 and (D) CDDP - pH 5.5. Each data point is presented as mean ± SD (n = 3), where no error bars are visible the SD was smaller than the symbols.

3.4. Cell Uptake

It was confirmed *in vitro,* using PSVue as a fluorescent reporter substance, that CHC nanoparticles improved cell internalization by stem-like A549-ON lung cancer cells and that the anti-CD133 modification enhanced the cell uptake even further, achieving an uptake ratio of 1.3 relative to free PSVue after 4 hours. It was further demonstrated that the uptake of anti-CD133

nanoparticles was significantly higher for the A549-ON cells compared to native A549 cells (Fig. 5).

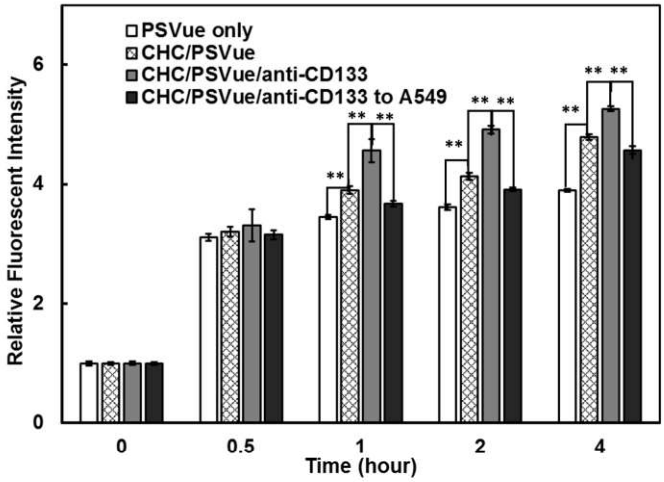

Fig. 5. *In vitro* cellular uptake of free PSVue, CHC/PSVue and CHC/PSVue/anti-CD133 nanoparticles by A549-ON cell after incubation for 0, 0.5, 1, 2 and 4 h. Uptake of CHC/PSVue/anti-CD133 by native A549 cells is included for comparison. Each data point is presented as mean ± SD (n = 3). Double-star (**) indicate significance (p-value <0.01).

3.5. In Vitro Cytotoxicity

In vitro cell assays revealed that CHC nanoparticles improved the cytotoxicity of DMC and CDDP against A549-ON and A549 cells. For A549-ON cells the IC_{50} values of free DMC, CHC/DMC, free CDDP and CHC/CDDP after 24 hours of incubation were calculated to 11, 6.0, 297 and 242 µg/mL (33, 18, 990 and 810 µM), respectively. The IC_{50} values against native A549 cells were determined to 11.8, 6.1, 124.9 and 33.1 (35, 18, 416 and 110 µM) for free DMC, CHC/DMC, free CDDP and CHC/CDDP, respectively (Table 2). The results highlight the resistance of A549-ON cells against CDDP. Furthermore, the increase in drug potency from encapsulation into the CHC nanoparticles was similar between the cell lines for DMC, while for

CDDP the result differed greatly between the cell lines. The encapsulation only resulted in a slight lowering of the IC_{50} value for A549-ON cells while the IC_{50} for native A549 cells was decreased from 124.9 µg/mL to 33.1 µg/mL.

Table 2. IC_{50} for treatment of A549 and A549-ON cells with DMC or CDDP as free drugs or in CHC nanoparticles.

Drug (µg/mL) / Cell line	DMC	CDDP	CHC-DMC	CHC-CDDP
A549	11.8	124.9	6.1	33.1
A549-ON	11	297	6.0	242

The synergy between DMC and CDDP as free drugs, in CHC nanoparticles and in CHC/anti-CD133 nanoparticles, was investigated utilizing a Chou-Talalay's Plot (Fa-CI plot) [18], shown in Fig. 6A. Briefly, on the Y-axis the combination index (CI) is shown for different concentrations of the two drugs, with the corresponding effects (Fa) being shown on the X-axis. CI values less than one, equal to one and more than one indicate synergistic, additive and antagonistic drug effects, respectively. Against A549-ON cells all concentrations of free DMC and CDDP were indicated to be antagonistic in their effects. In contrast, when loaded into CHC nanoparticles synergy was observed for high Fa, i.e., the two dual-drug combinations with highest concentration ([DMC] = 6 and 9 µg/mL; [CDDP] = 250 and 265 µg/mL). When loaded into the CD133-targeted CHC nanoparticles even stronger synergistic effect was observed at even lower Fa, i.e., starting at lower drug concentrations ([DMC] = 5 µg/mL and [CDDP] = 200 µg/mL). In contrast to the results for MDR A549-ON cells, for native A549 cells similar degree of synergy was observed both for free drugs and drugs loaded in the CHC/DMC-CDDP

nanoparticles, with free drugs even presenting higher degree of synergy at the lowest concentrations (Fig. S3). The degree to which the targeting increased cytotoxicity of the dual-loaded drugs against MDR A549-ON cells is also clear when comparing the cell viability after exposure to different drug concentrations from CHC/DMC-CDDP or CHC/DMC-CDDP/anti-CD133 nanoparticles for 24h.

As seen in Fig. 6B the cell killing was much improved even at lower concentrations for the targeted nanoparticles, as compared to the non-targeted ones. At the highest investigated concentration of drugs ([DMC] = 9 μg/mL and [CDDP] = 265 μg/mL) the cell viability was as low as 4% for CHC/DMC-CDDP/anti-CD133 while it was 23% for CHC/DMC-CDDP. Control experiments using CHC or CHC/anti-CD133 nanoparticles without drugs revealed that both nanoparticles presented negligible effect on cell viability of A549-ON cells (Fig. S2).

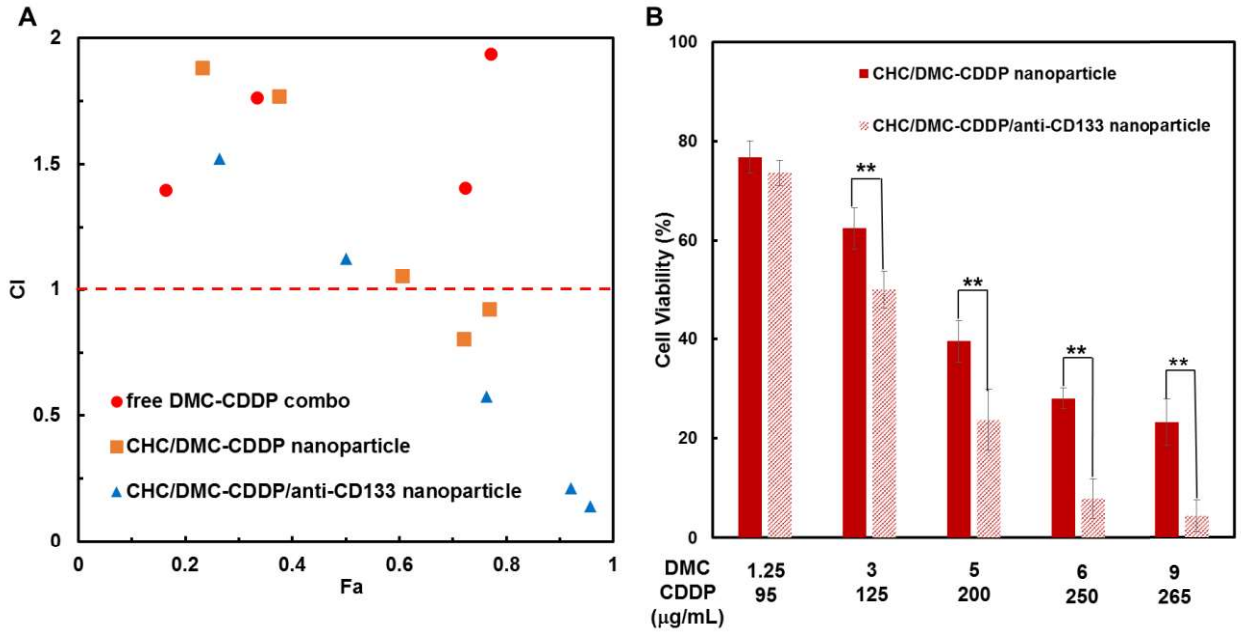

Fig. 6. *In vitro* cytotoxicity of A549-ON treated with various drug combinations for 24 hours. (A) The Chou-Talalay's Plot for A549-ON cells treated with free dual drugs, CHC/dual-drug nanoparticles and CHC/dual-drug/anti-CD133 nanoparticles for 24 hrs. (B)The cell viability of

A549-ON cells treated with different dosages of CHC/dual-drug nanoparticles and CHC/dual-drug/anti-CD133 nanoparticles for 24 hrs. Each data point is presented as mean ± SD (n = 3). The double-star (**) indicate significance (p-value <0.01).

4. Discussion

CHC nanoparticles loaded with the dual drugs DMC and CDDP and modified with antibodies for targeting of the CSC surface marker CD133 (CHC/DMC-CDDP/anti-CD133) were successfully prepared by a one-pot synthesis at room temperature in water, involving only small amounts of the benign solvent DMSO. The nanoparticles achieved greatly increased synergy between the drugs in vitro. The feasible preparation was ascribed to the fact that CHC presents nano-microenvironments that can house both hydrophilic and hydrophobic substances [25]. As discussed in section 3.1 and shown from analyses (Fig. 1 and 2) the hydrophilic CDDP became chemically bound to carboxylic acid oxygens of CHC, which explains the effective and stable loading of this hydrophilic substance. The subsequent controlled release of CDDP was explained by replacement of the carboxylic acid ligands of CHC with water or chloride [22]. Although CDDP is highly water soluble EE of up to 60% was achieved during dual-drug loading in aqueous solution and only about 14% of the drug was released during *in vitro* release studies in PBS with pH = 7.4 (Fig. 4C). For DMC the low chemical potential in the hydrophobic domains of CHC nanoparticles, compared to in water (very low water solubility), was enough to achieve stable drug loading and controlled release. The EE for DMC in the dual-drug loaded particles was up to 50% and only about 10% of the drug was released during the *in vitro* release studies in PBS with pH = 7.4 (Fig. 4A). The high EE for both drugs and the very limited escape of the drugs at pH 7.4 indicated that the CHC nanoparticles would retain the drug in

circulation/extracellular space, offering potential for simultaneous delivery of the drugs after internalization by cells in endo/lysosomes. It was found that the amounts of released drugs increased slightly at pH 5.5, but 70% and 80% still remained in the nanoparticles for CDDP and DMC, respectively (Fig. 4B, D). It was thus concluded that the drug loading in the particles was highly stable and even under lysosome-relevant pH of 5.5 drug release by passive diffusion out from the particles would be marginal. However, from our previous work it was known that CHC is degraded by lysozyme [20, 21]. It was expected that intracellular release would be triggered to some extent by this enzymatic degradation once the nanoparticles had been internalized by the cells and ended up in endosomes or lysosomes [21], ensuring simultaneous intracellular delivery of both drugs at accelerated release rate for enhanced synergistic effect.

Evaluation of different preparations of the drugs and CHC nanoparticles, with/without CD133-targeting, in cell assays using highly malignant and MDR A549-ON lung CSC [9, 10] revealed that CD-133 targeting modification corresponded with increased cell uptake and that uptake of the targeted nanoparticles was higher by A549-ON cells than by native A549 cells (Fig. 5). Furthermore, the CHC/DMC-CDDP/anti-CD133 nanoparticles greatly enhanced the synergistic effects between the drugs against MDR A549-ON (Fig. 6), while against native non-MDR A549 cells the synergy was comparable between free drugs and drugs loaded in the functionalized nanoparticles (Fig. S3). This is in contrast to a recent study in which no improvement (possibly some reduction) in combined cytotoxicity was observed *in vitro* for combinations of CDDP/polymer-conjugated nanoparticles and free curcumin against CDDP-resistant ovarian cells, compared to when using combinations of the free drugs at the same concentrations [14]. Likely the greatly improved synergy by CHC/DMC-CDDP/anti-CD133 nanoparticles in the present study was due to effective cell internalization and simultaneous intracellular release of

the two drugs, which in turn enabled suppression of MDR and effective cell killing (see Scheme 2). However, it is recognized that the increase in cell uptake with the anti-CD133 modification was moderate and likely there were additional underlying mechanisms that contributed to the greatly enhanced synergy. Those mechanisms and detailed cell-biological responses to the CHC/DMC-CDDP/anti-CD133 nanoparticles would be an interesting topic for a future study.

The outstanding degree to which the CHC/DMC-CDDP/anti-CD133 nanoparticles mediated synergy between DMC and CDDP becomes further evident by comparing their cytotoxicity against the A549-ON cells after 24 h with that of dual-administered free drugs at similar drug concentrations. For example, for administration of 15 μg/mL of DMC and 300 μg/mL CDDP as free drugs the cell viability was about 28% after 24 h, while for administration of 9 μg/mL of DMC and 265 μg/mL CDDP in CD133-targeting CHC nanoparticles the viability was as low as 4% (Fig. S4). Further indication of the potency of the CHC/DMC-CDDP/anti-CD133 nanoparticle system against the MDR A549-ON lung CSC is given by comparing the cytotoxicity at a CDDP concentration similar to the IC_{50} concentrations of free CDDP and CDDP/CHC, which were 297 and 242 μg/mL, respectively. At a similar CDDP concentration of 265 μg/mL the CHC/DMC-CDDP/anti-CD133 with 9 μg/mL DMC all but eradicated the A549-ON cells. This is especially impressive given that the viability of CDDP-resistant A549 cells has been found to plateau at a viability of about 40% with increasing CDDP concentration [26] and that in another study the inhibition was only about 40% when such cells were incubated with 200 μg/mL CDDP for 24 h [27]. The ability of the CHC/DMC-CDDP/anti-CD133 nanoparticle system to kill close to all cancer cells is highly relevant for improved treatments as it is considered that in the clinic insufficient killing of tumors may result in cancer relapse with cells having pre-existing or acquired drug resistance.

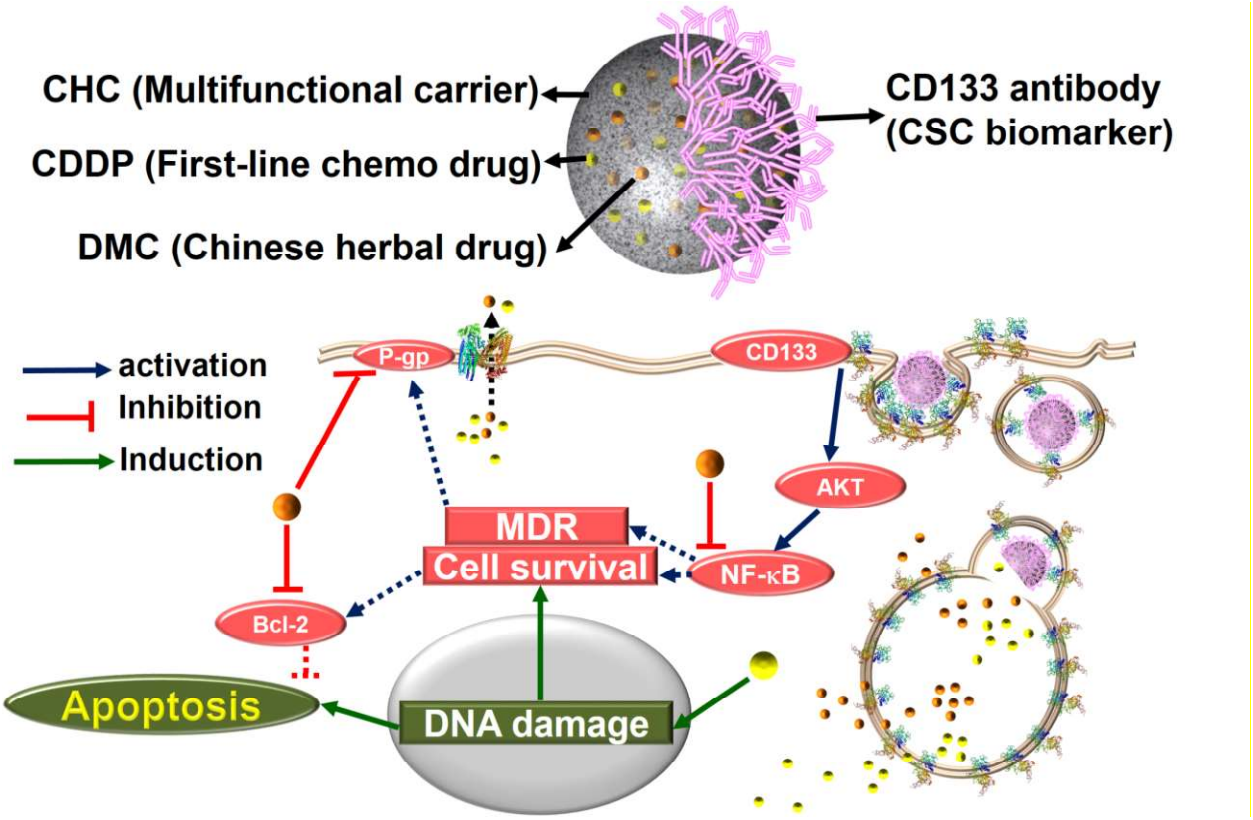

Scheme 2. Illustration of how the CHC/DMC-CDDP/anti-CD133 nanoparticles enter the cells and how the drugs act in synergy to overcome MDR.

With regard to opportunities to formulate the nanoparticles for clinical administration; the size and zeta potential analyses revealed sizes < 200 nm and a slightly negative zeta potential of -3 mV for the CHC/DMC-CDDP/anti-CD133 nanoparticles (Fig. 3 and Table 1). Such size and zeta potential indicate promise for circulating nanoparticles targeting the leaky vasculature in vicinity of tumors [28], i.e., the EPR-effect. Although, since the focus of the system is lung cancer, direct administration to cancerous lung tissue or lymph nodes via inhalation [29-31] and injection [32] are also interesting opportunities to consider when developing and formulating the particles for further evaluation in disease relevant models.

To conclude, the outstanding efficacy of the CHC/DMC-CDDP/anti-CD133 nanoparticles against stem-like lung cancer cells, highly feasible one-pot preparation, colloidal properties and previously demonstrated biodegradation and biocompatibility of CHC [19, 20] indicate that the system has clear potential as a dual-drug nanomedical approach to battle multidrug resistant lung cancer, including the elusive stem-like cancer cells. Further investigations using an *in-vivo* lung tumor model is currently under development for this dual-drug biofunctionalized CHC nanoparticle technology and will be reported separately.

Acknowledgements

Sincere thanks to Prof. Hui-Yi Lin, China Medical University, Taiwan, for providing the DMC. Heartfelt thanks to Prof. Shih-Hwa Chiou, Yang Ming University, Taiwan, for providing the A549-ON cell line. The financial support of this work by the University System of Taiwan (Taiwan) and Taipei Veterans General Hospital (Taiwan), under contract number: 103W933, is gratefully acknowledged

References

[1] American Cancer Society Homepage - Chemotherapy for non-small cell lung cancer. http://www.cancer.org/cancer/lungcancer-non-smallcell/detailedguide/non-small-cell-lung-cancer-treating-chemotherapy (accessed October 13, 2016).

[2] American Cancer Society. Cancer Facts & Figures 2016. Atlanta: American Cancer Society; 2016.

[3] Cojoc M, Mäbert K, Muders MH, Dubrovska A. A role for cancer stem cells in therapy resistance: Cellular and molecular mechanisms. Seminars in Cancer Biology 2015;31:16-27.

[4] Zakaria N, Yusoff NM, Zakaria Z, Lim MN, Baharuddin PJN, Fakiruddin KS, et al. Human non-small cell lung cancer expresses putative cancer stem cell markers and exhibits the transcriptomic profile of multipotent cells. BMC Cancer 2015;15:1-16.

[5] Gadde S. Multi-drug delivery nanocarriers for combination therapy. MedChemComm 2015;6:1916-29.

[6] Stewart DJ. Mechanisms of resistance to cisplatin and carboplatin. Critical Reviews in Oncology / Hematology;63:12-31.

[7] Chen J, Solomides C, Parekh H, Simpkins F, Simpkins H. Cisplatin resistance in human cervical, ovarian and lung cancer cells. Cancer Chemotherapy and Pharmacology 2015;75:1217-27.

[8] Xi G, Hayes E, Lewis R, Ichi S, Mania-Farnell B, Shim K, et al. CD133 and DNA-PK regulate MDR1 via the PI3K- or Akt-NF-[kappa]B pathway in multidrug-resistant glioblastoma cells in vitro. Oncogene 2016;35:241-50.

[9] Chiou S-H, Wang M-L, Chou Y-T, Chen C-J, Hong C-F, Hsieh W-J, et al. Coexpression of Oct4 and Nanog Enhances Malignancy in Lung Adenocarcinoma by Inducing Cancer Stem Cell–Like Properties and Epithelial–Mesenchymal Transdifferentiation. Cancer Research 2010;70:10433-44.

[10] Chen Y-C, Hsu H-S, Chen Y-W, Tsai T-H, How C-K, Wang C-Y, et al. Oct-4 Expression Maintained Cancer Stem-Like Properties in Lung Cancer-Derived CD133-Positive Cells. PLoS One 2008;3:e2637.

[11] Olivera A, Moore TW, Hu F, Brown AP, Sun A, Liotta DC, et al. Inhibition of the NF-κB signaling pathway by the curcumin analog, 3,5-Bis(2-pyridinylmethylidene)-4-piperidone (EF31): anti-inflammatory and anti-cancer properties. International Immunopharmacology 2012;12:368-77.

[12] Anand P, Sundaram C, Jhurani S, Kunnumakkara AB, Aggarwal BB. Curcumin and cancer: An "old-age" disease with an "age-old" solution. Cancer Letters 2008;267:133-64.

[13] Chen P, Li J, Jiang H-G, Lan T, Chen Y-C. Curcumin reverses cisplatin resistance in cisplatin-resistant lung caner cells by inhibiting FA/BRCA pathway. Tumor Biology 2014;36:3591-9.

[14] Kang X, Zhao C, Yan L, Qi R, Jing X, Wang Z. Sensitizing nanoparticle based platinum(IV) drugs by curcumin for better chemotherapy. Colloids and Surfaces B: Biointerfaces 2016;145:812-9.

[15] Quitschke WW. Differential solubility of curcuminoids in serum and albumin solutions: implications for analytical and therapeutic applications. BMC Biotechnology 2008;8:1-17.

[16] Moura MJ, Gil MH, Figueiredo MM. Delivery of cisplatin from thermosensitive co-cross-linked chitosan hydrogels. European Polymer Journal 2013;49:2504-10.

[17] Song W, Tang Z, Zhang D, Zhang Y, Yu H, Li M, et al. Anti-tumor efficacy of c(RGDfK)-decorated polypeptide-based micelles co-loaded with docetaxel and cisplatin. Biomaterials 2014;35:3005-14.

[18] Chou T-C. Theoretical Basis, Experimental Design, and Computerized Simulation of Synergism and Antagonism in Drug Combination Studies. Pharmacological Reviews 2006;58:621-81.

[19] Hsiao M-H, Chiou S-H, Larsson M, Hung K-H, Wang Y-L, Liu CJ-L, et al. A temperature-induced and shear-reversible assembly of latanoprost-loaded amphiphilic chitosan colloids: Characterization and in vivo glaucoma treatment. Acta Biomaterialia 2014;10:3188-96.

[20] Chou H-S, Larsson M, Hsiao M-H, Chen Y-C, Röding M, Nydén M, et al. Injectable insulin-lysozyme-loaded nanogels with enzymatically-controlled degradation and release for basal insulin treatment: In vitro characterization and in vivo observation. Journal of Controlled Release 2016;224:33-42.

[21] Huang W-T, Larsson M, Wang Y-J, Chiou S-H, Lin H-Y, Liu D-M. Demethoxycurcumin-Carrying Chitosan–Antibody Core–Shell Nanoparticles with Multitherapeutic Efficacy toward Malignant A549 Lung Tumor: From in Vitro Characterization to in Vivo Evaluation. Molecular Pharmaceutics 2015;12:1242-9.

[22] Yan X, Gemeinhart RA. Cisplatin delivery from poly(acrylic acid-co-methyl methacrylate) microparticles. Journal of Controlled Release 2005;106:198-208.

[23] Brière MK, Goel R, Shirazi HF, Stewart JD, Smith PIC. The integrity of cisplatin in aqueous and plasma ultrafiltrate media studied by 195Pt and 15N nuclear magnetic resonance. Cancer Chemotherapy and Pharmacology;37:518-24.

[24] Silva H, Barra CV, Rocha FV, Frézard F, Lopes MTP, Fontes APS. Novel platinum(II) complexes of long chain aliphatic diamine ligands with oxalato as the leaving group: comparative cytotoxic activity relative to chloride precursors. Journal of the Brazilian Chemical Society 2010;21:1961-7.

[25] Larsson M, Huang W-C, Hsiao M-H, Wang Y-J, Nydén M, Chiou S-H, et al. Biomedical applications and colloidal properties of amphiphilically modified chitosan hybrids. Progress in Polymer Science 2013;38:1307-28.

[26] Barr MP, Gray SG, Hoffmann AC, Hilger RA, Thomale J, O'Flaherty JD, et al. Generation and Characterisation of Cisplatin-Resistant Non-Small Cell Lung Cancer Cell Lines Displaying a Stem-Like Signature. PLoS One 2013;8:e54193.

[27] Zeng H-Z, Qu Y-Q, Zhang W-J, Xiu B, Deng A-M, Liang A-B. Proteomic Analysis Identified DJ-1 as a Cisplatin Resistant Marker in Non-Small Cell Lung Cancer. Int J Mol Sci 2011;12:3489.

[28] Wang AZ, Langer R, Farokhzad OC. Nanoparticle Delivery of Cancer Drugs. Annual Review of Medicine 2012;63:185-98.

[29] Garbuzenko OB, Mainelis G, Taratula O, Minko T. Inhalation treatment of lung cancer: the influence of composition, size and shape of nanocarriers on their lung accumulation and retention. Cancer Biology & Medicine 2014;11:44-55.

[30] Kim I, Byeon HJ, Kim TH, Lee ES, Oh KT, Shin BS, et al. Doxorubicin-loaded highly porous large PLGA microparticles as a sustained- release inhalation system for the treatment of metastatic lung cancer. Biomaterials 2012;33:5574-83.

[31] Choi SH, Byeon HJ, Choi JS, Thao L, Kim I, Lee ES, et al. Inhalable self-assembled albumin nanoparticles for treating drug-resistant lung cancer. J Controlled Release 2015;197:199-207.

[32] Hohenforst-Schmidt W, Zarogoulidis P, Darwiche K, Vogl T, Goldberg EP, Huang H, et al. Intratumoral chemotherapy for lung cancer: re-challenge current targeted therapies. Drug Des Devel Ther 2013;7:571-83.